

# icaeyeblinkmetrics()

This EEGLAB toolbox is designed for automated/semi-automated selection of ICA components associated with eye-blink artifact using time-domain measures. The toolbox is based on the premises that 1) an ICA component associated with eye blinks should be more related to the recorded eye blink activity than other ICA components, and 2) removal of the ICA component associated with eye blinks should reduce the eye blink artifact present within the EEG following back projection.

Other than the EEG input, the only required input for the function is specification of the channel that exhibits the artifact (in most cases the VEOG electrode). This can either be stored within the EEG.data matrix or within EEG.skipchannels. It will then identify eye-blanks within the channel to be used for computation of the metrics listed below. If you are not sure what channel to choose, you can let the function determine the channel where the artifact maximally presents but this does slow the function down.

**The toolbox does not change the data in any way**, it only provides an output stored in 'EEG.icaquant' providing:

1. Metrics:
  - a. The correlation between the measured artifact in the artifact channel and each ICA component. (i.e. how similar the ICA component is to the eye blink)
  - b. The adjusted normalized convolution of the ICA component activity with the measured artifact in the artifact channel. (i.e., how well does the ICA component overlap with the eye blink)
  - c. The percent reduction in the artifact present in the EEG for each ICA component if it was removed. (i.e., how much is the eye blink artifact reduced in the EEG when the component is removed)
2. Identified Components: the ICA components that exhibit statistically significant values for all three metrics. Alpha defaults to  $p \leq 0.001$ .
3. Artifact Latencies: the latencies that were used in the computation of the metrics.

## Release Notes:

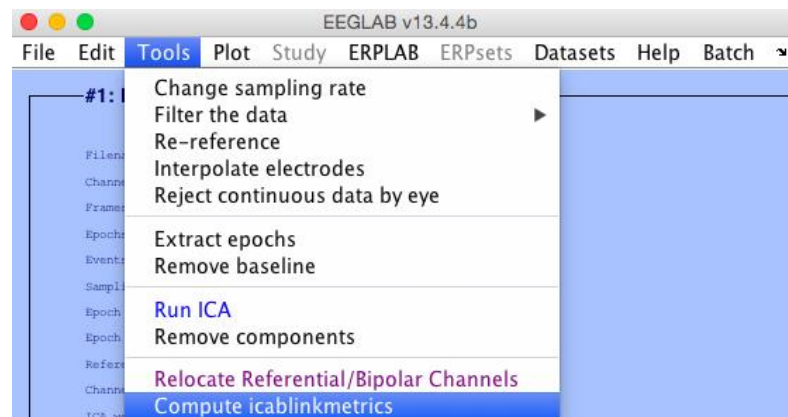
### Version 3.0

- Updated eyeblinklatencies() code to increase computational speed. Default threshold was lowered to correlation of 0.96 based upon updates to the implementation approach. Added parameter to allow for inputting a user specified template for eye blink identification. For older Matlab versions, that may not allow for the new approach, the old implementation is retained.
- Updated icablinkmetrics() code to increase computational speed. Added catch to reduce correlation threshold for eyeblinklatencies() to 0.9 if too few eye blinks are identified. Reduced the volume of content written to the Matlab window.

## Example Implementation Using the Tools menu of EEGLAB

Step 1: Open a continuous EEG dataset that has had ICA weights computed (i.e., EEG.icaweights should not be empty).

Step 2: Using the EEGLAB Graphical User Interface, click on the Tools menu, Then select 'Compute icablinkmetrics'

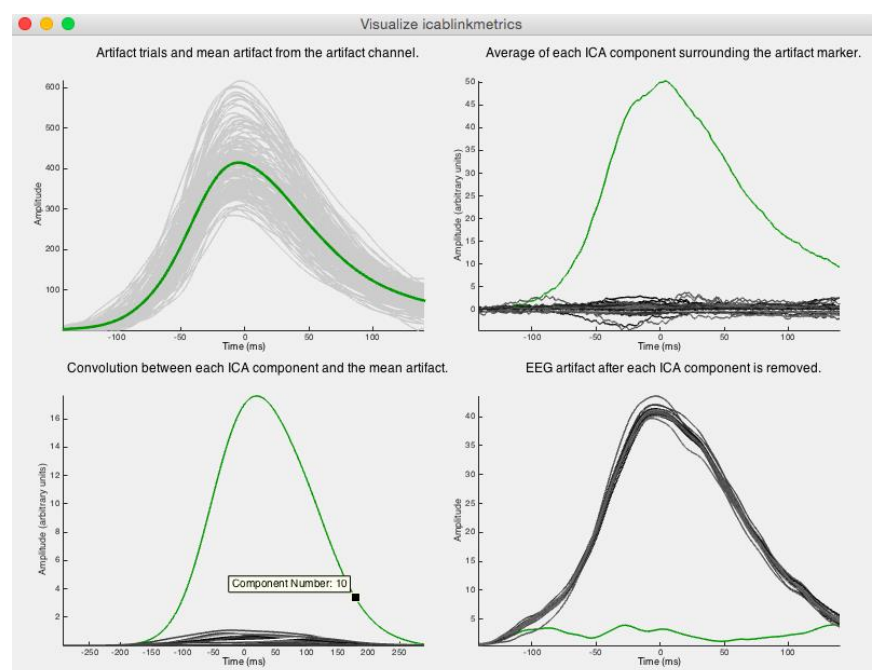
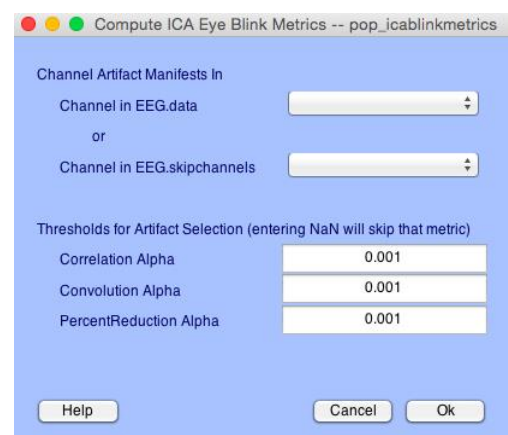


Step 3: A separate Graphical User Interface will pop up asking you to select the channel where the eye blink artifact manifests. This is typically your VEOG channel, but any channel where the eye blink artifact clearly presents should work (i.e., FP1). If the channel is included in the EEG.data, select from that option box. If the data has been relocated to EEG.skipchannels, there is a separate option box to select from.

Step 4: Specify the Alpha criterion necessary for selection of a component. The default is  $p \leq 0.001$  which is applied globally, but the criterion can be applied differentially for each metric. Only those components which exhibit statistically significant values below the criterion will be identified.

Step 5: After the function has identified eye blink artifacts in the specified channel and then computed the metrics, it will display time-series plots showing the mean and individual trials for the eye blinks (upper left); the mean of each ICA component in the period surrounding the eye blinks (upper right); the convolution between each mean ICA component and the mean artifact (lower left); and the mean EEG data in the period surrounding the eye blinks when each component is removed (lower right). Clicking on a line will provide a tooltip displaying the component number.

Step 6: The Command Window will also display the identified component (plotted in the figure in green) and the location where the blink metrics were stored in the EEG structure.



## Example Implementation Code Using Command Window

```
clear; clc; % Clear memory and the command window
eeglab; % Start eeglab: Requires Matlab Signal Processing Toolbox & Statistics Toolbox

filelocation = '/Studies/'; % Establish path to where the SET file is located

%% Prepare Data for ICA computation
% Read in a continuous EEG dataset with any bad channels/segments removed
EEG = pop_loadset('filename','RawEEG.set','filepath',filelocation); EEG = eeg_checkset(EEG);

% Remove additional data points 2 seconds outside of triggers
winPadding = 2;
winStart = (EEG.event(1).latency-(EEG.srate*((1000/EEG.srate)*winPadding)));
winStop = (EEG.event(end).latency+(EEG.srate*((1000/EEG.srate)*winPadding)));
if (winStart < 1); winStart = 1; end; if (winStop > EEG.pnts); winStop = EEG.pnts; end;
EEG = pop_select( EEG, 'point', [winStart, winStop]); EEG = eeg_checkset(EEG);

% HighPass Filter the data to remove slow drift
EEG = pop_basicfilter(EEG,1:size(EEG.chanlocs,2),'Filter','highpass',...
    'Design','butter','Cutoff',0.05,'Order',2,'Boundary',87);

% Relocate referential/bipolar channels so they can be recovered later if necessary
EEG = movechannels(EEG,'Location','skipchannels','Direction','Remove',...
    'Channels',{'M1','M2','VEOG','HEOG'});

% Compute ICA
EEG = pop_runica(EEG, 'icatype', 'runica', 'options', ...
    {'extended',1,'block',floor(sqrt(EEG.pnts/3)),'anneal',0.98});
EEG = eeg_checkset(EEG);

%% icablinkmetrics implementation
% Find Eye Blink Component(s)
EEG.icaquant = icablinkmetrics(EEG,'ArtifactChannel',...
    EEG.skipchannels.data(find(strcmp({EEG.skipchannels.labels}, 'VEOG'))),:,'VisualizeData','True');

disp('ICA Metrics are located in: EEG.icaquant.metrics')
disp('Selected ICA component(s) are located in: EEG.icaquant.identifiedcomponents')
[~,index] = sortrows([EEG.icaquant.metrics.convolution].');
EEG.icaquant.metrics = EEG.icaquant.metrics(index(end:-1:1)); clear index

% Remove Artifact ICA component(s)
EEG = pop_subcomp(EEG,EEG.icaquant.identifiedcomponents,0);
```

# Evaluating the efficacy of fully automated approaches for the selection of eyeblink ICA components

MATTHEW B. PONTIFEX ,<sup>a</sup> VLADIMIR MISKOVIC,<sup>b</sup> AND SARAH LASZLO<sup>b</sup>

<sup>a</sup>Department of Kinesiology, Michigan State University, East Lansing, Michigan, USA

<sup>b</sup>Department of Psychology, Binghamton University, Vestal, New York, USA

## Abstract

Independent component analysis (ICA) offers a powerful approach for the isolation and removal of eyeblink artifacts from EEG signals. Manual identification of the eyeblink ICA component by inspection of scalp map projections, however, is prone to error, particularly when nonartifactual components exhibit topographic distributions similar to the blink. The aim of the present investigation was to determine the extent to which automated approaches for selecting eyeblink-related ICA components could be utilized to replace manual selection. We evaluated popular blink selection methods relying on spatial features (EyeCatch), combined stereotypical spatial and temporal features (ADJUST), and a novel method relying on time series features alone (icablinkmetrics) using both simulated and real EEG data. The results of this investigation suggest that all three methods of automatic component selection are able to accurately identify eyeblink-related ICA components at or above the level of trained human observers. However, icablinkmetrics, in particular, appears to provide an effective means of automating ICA artifact rejection while at the same time eliminating human errors inevitable during manual component selection and false positive component identifications common in other automated approaches. Based upon these findings, best practices for (a) identifying artifactual components via automated means, and (b) reducing the accidental removal of signal-related ICA components are discussed.

**Descriptors:** Independent component analysis, EEG artifact, EEGLAB

Over the past decade, an increasing number of laboratories have begun to utilize temporal independent component analysis (ICA) to isolate and remove eyeblink artifacts from EEG signals. Indeed, examination of the journal *Psychophysiology* over the past 2 years reveals that nearly the same proportion of EEG investigations utilize temporal ICA approaches for eyeblink artifact reduction/correction as those investigations that utilize regression-based approaches. This is undoubtedly related in some part to the growing adoption of EEGLAB (Delorme & Makeig, 2004), a MATLAB/octave-based graphical toolbox for data processing that implements temporal ICA in its standard workflow. Of practical importance, this temporal ICA approach to artifact correction may not be globally appropriate for all artifacts—such as saccadic eye movements and nonstationary artifacts, (see Hoffmann & Falkenstein, 2008, for further discussion). However, for eyeblink artifact correction, the ICA approach has been found to exhibit superior performance relative to regression-based approaches (Jung et al.,

2000). An important distinction to make, however, is that, unlike regression-based approaches, ICA does not inherently perform any form of artifact correction. That is, these approaches are simply blind-source signal separation techniques that attempt to dissociate temporally independent yet spatially fixed components (Bell & Sejnowski, 1995). Thus, a critical limitation of temporal ICA-based approaches to artifact correction is the reliance on subjective human judgments to determine what components are associated with noise rather than signal, so that the data can be back-projected to reconstruct EEG signals in the absence of artifactual activity. Although automated approaches exist, we have little understanding of the extent to which these automated ICA component selection approaches are robust to variation in signal-to-noise ratio or across varying electrode densities. Thus, the aim of the present investigation was to determine if fully automated approaches for selecting eyeblink-related ICA components can and should be utilized to replace manual selection of eyeblink artifact components by human users.

In a common EEGLAB workflow, following separation of the signals using standard ICA algorithms, a human observer must visually sift through the full set of temporal ICA components in order to manually select one or more components for removal. Such an approach is not only labor intensive, but it is also user dependent, making it more prone to errors or, potentially, to bias (e.g., quality control is dependent on the user's expertise level).

Support for the preparation of this manuscript was provided by a grant from the Eunice Kennedy Shriver National Institute of Child Health and Human Development (NICHD) to MBP (R21 HD078566), and by grants from the National Science Foundation (NSF) to SL (NSF CAREER-1252975, NSF TWC SBE-1422417, and NSF TWC SBE-1564046).

Address correspondence to: Matthew B. Pontifex, Ph.D., Department of Kinesiology, 27P IM Sports Circle, Michigan State University, East Lansing, MI 48824-1049, USA. E-mail: pontifex@msu.edu

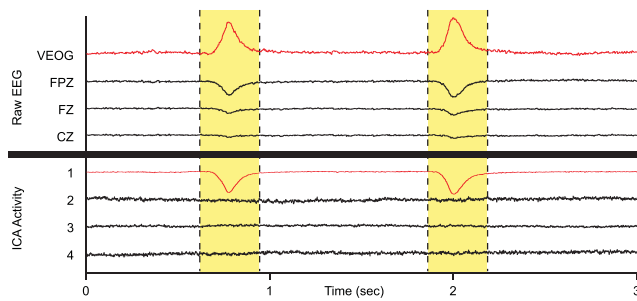


**Figure 1.** Illustration of eyeblinks recorded from the VEOG electrode, how they manifest across three midline electrode sites, and how the eyeblink-related signal is separated from other signals using ICA decomposition. Note the high degree of similarity between the VEOG electrode and ICA component 1.

Human fallibility is especially relevant in the case of experiments concerned with frontal ERP/EEG activity, where it is particularly difficult to differentiate the scalp projection of the temporal ICA component(s) associated with eyeblink activity from the scalp projection of the temporal ICA component(s) associated with genuine, frontally maximal cortical activity, such as the LAN (left anterior negativity; Castellanos & Makarov, 2006). Although it is possible to inform these decisions by inspecting temporal ICA activations (see Figure 1), such approaches are not explicitly detailed within the EEGLAB documentation, rendering knowledge and implementation of such methodologies potentially variable across research laboratories.

To address the potential limitations of human-selected ICA artifact rejection, a number of methods for automatic identification of artifact-related temporal ICA components have been developed for EEGLAB. These include ADJUST (Mognon, Jovicich, Bruzzone, & Buiatti, 2011), CORRMAP (Viola, Thorne, Edmonds, Schneider, & Eichele, 2009), and EyeCatch (Bigdely-Shamlo, Kreutz-Delgado, Kothe, & Makeig, 2013). It should be pointed out that such approaches are simply added on following the application of ICA to the data in order to automate the selection of artifact-related components, and are not used as a replacement for the ICA application. The most widely downloaded software plugin is the ADJUST method, which attempts to identify a wide array of potential sources of artifact such as eyeblinks, eye movements, cardiac-induced artifacts, and other stereotypical movements. To this end, temporal independent components are characterized by combining both spatial and temporal information, with the identification of artifactual components based on stereotyped spatiotemporal features such as temporal kurtosis and the spatial average difference. Alternatively, the Eye-Catch plugin attempts to distinguish temporal ICA components based on the correlation between the scalp map projection for each ICA component and a database of 3,452 (as of the writing of this manuscript) exemplar eye activity-related template scalp maps. This approach has been found to exhibit overall performance similar to the CORRMAP function (Viola et al., 2009) but has an advantage over CORRMAP in that it is fully automated.

A limitation of the approaches mentioned above is that they largely rely on ancillary indices of ICA components, such as scalp map projections of temporal ICA weights, to differentiate eyeblink-related components from nonblink-related components, rendering them prone to the same potential sources of error as the human visual inspection approach—particularly when nonartifactual frontally maximal ICA components occur. Since these approaches rely on the scalp topography of the temporal ICA components, the eyeblink component can easily be confused with

nonartifactual frontally distributed components. This is a fundamental weakness of any topography-based approach to selecting the eyeblink-related temporal ICA component. In contrast, a time-domain approach should not be vulnerable to potential confusion between frontally distributed nonartifact components and eyeblink-related components. Accordingly, we were interested in comparing a time-domain approach to the existing spatial approaches. Consequently, we developed a time-domain approach, icablinkmetrics, predicated on two basic premises: (1) that the temporal ICA component(s) associated with eyeblinks should be related to the eyeblink activity present within the EEG more so than any other temporal ICA component (e.g., via correlation and convolution), and (2) that removal of the temporal ICA component associated with the eyeblinks should reduce the eyeblink artifact present within the EEG data more so than the removal of any other temporal ICA component following back projection (when the data is reconstructed without the artifactual component). Again, this approach is simply added on following the application of ICA to the data in order to automate the selection of artifact-related components, and is not used as a replacement to the ICA application. For a more detailed description of the background and theory underlying the premises that guided the development of the icablinkmetrics time-domain approach, see the online supporting information Appendix S1. In the interest of transparency, we note that the icablinkmetrics approach was created by author MBP with input from SL. The icablinkmetrics EEGLAB plugin—which can be run from either the command line or the Tools menu of EEGLAB—is available through the EEGLAB Extension Manager or by downloading from [http://sccn.ucsd.edu/wiki/EEGLAB\\_Extensions](http://sccn.ucsd.edu/wiki/EEGLAB_Extensions).

The aim of the present investigation was to assess the efficacy of these automated approaches for the selection of eyeblink-related artifact components. To this end, we evaluated the relative merits of automatic approaches to eyeblink component selection methods relying on time series data (icablinkmetrics) as compared to those relying on combined stereotypical spatial and temporal features (ADJUST, Mognon et al., 2011) or spatial features alone (Eye-Catch, Bigdely-Shamlo et al., 2013). An intrinsic weakness of a temporal approach to eyeblink-related component selection is that, with increasing noise in the time series, procedures for identifying when eyeblink-related activity occurs are more prone to failure. To examine this issue, we utilized simulated EEG data to investigate the extent to which each of these automated approaches would be sensitive to variation in the magnitude of the eyeblink artifact amid increasing levels of noise in the signal. Next, we assessed the generalizability of these automated approaches across real EEG data collected with varying electrode densities and in response to different tasks. Finally, for comparison, we assessed the accuracy of the current common method of trained observers visually selecting temporal ICA components. Collectively, these analyses serve to address the critical question of whether fully automated approaches for selecting eyeblink-related ICA components can and should be utilized to replace manual selection of eye artifact components by human users and, if so, what their potential vulnerabilities are.

### Simulated EEG Varying in the Magnitude of the Artifact and Level of Noise

#### Method

A total of 3,072 simulated EEG data sets was created matched to three (real) exemplar EEG data sets (1,024 simulations per exemplar data set). For each exemplar data set, simulated data were

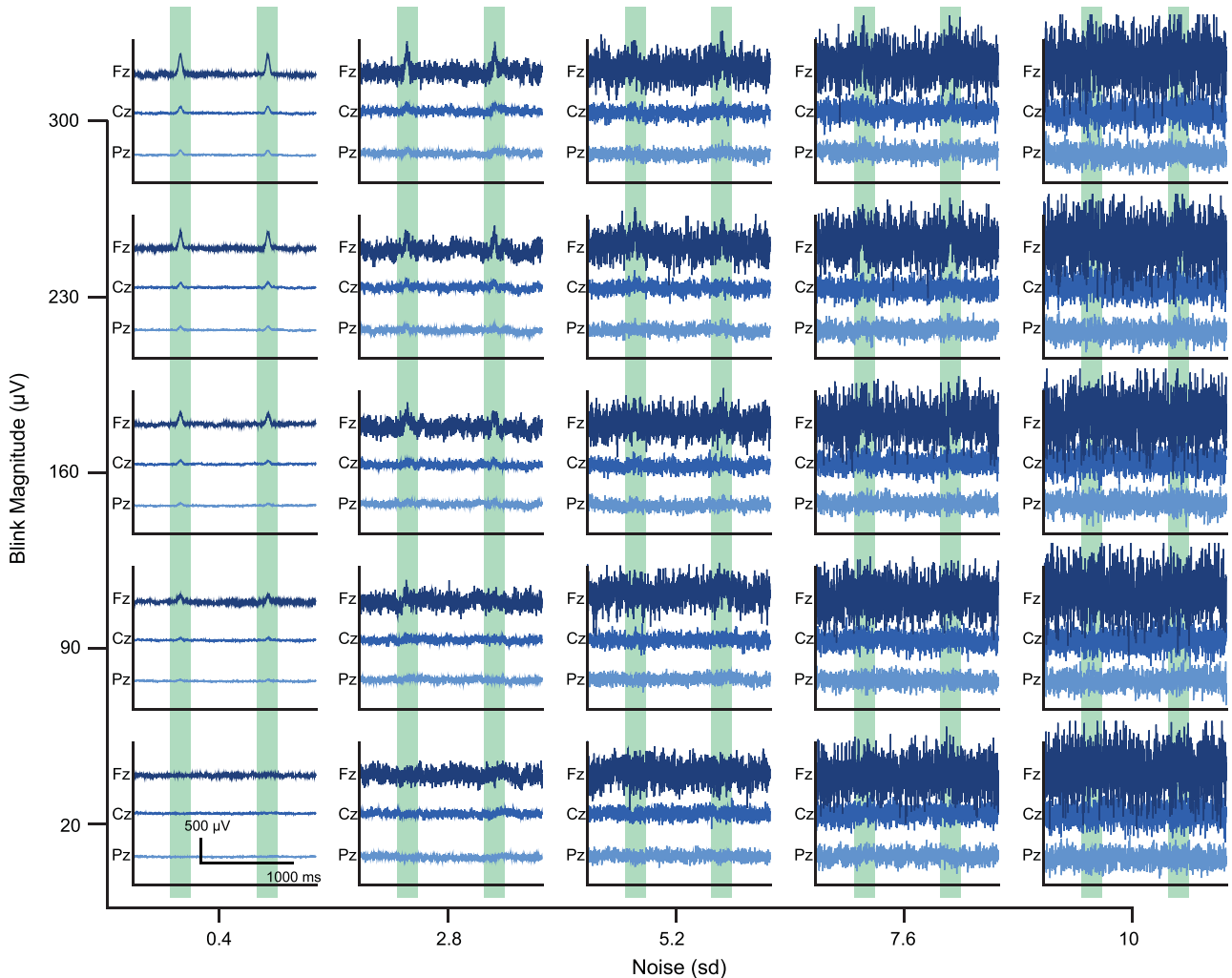


**Figure 2.** Representative data illustrating the simulated EEG across the range of possible eyeblink artifact magnitude and noise conditions for three electrode sites. For reference, the time points for the seeded eyeblinks are highlighted in green.

created representing a wide range of possible eyeblink artifact magnitude and noise conditions. In this context, the aim was not to simulate the computational processes by which the EEG signal is actually created in the brain (e.g., Laszlo & Armstrong, 2014; Laszlo & Plaut, 2012). Rather, our goal was to ensure that the artificial data exhibited the same frequency domain properties and signal-to-noise ratio (prior to the injection of more noise per the experimental manipulations) in the same amplitude range as true EEG data. Such an approach enabled the creation of EEG data sets that had similar properties to real EEG, while allowing for the ability to modulate the level of noise present within the signal as a function of the variability found within real EEG data sets. Simulated EEG data sets were created by (1) Fourier decomposing each exemplar data set at each channel, and then (2) producing weighted sums of sines with random phase shifts that resulted in simulated data sets with the same frequency characteristics as the exemplar. The first and last 100 points of the simulated time series were removed to account for edge artifacts from the finite sum of sines, and simulated time series were scaled to have the same mean and standard deviation as the exemplar data sets, per channel. Each simulated data set contained 25,480 points for each of 28 channels, allowing 32.5 data points for each ICA weight (data points/channels<sup>2</sup>). Noise was added to the simulated data sets by randomly perturbing both the phase and

amplitude at each point in the time series. Phase perturbations were distributed uniformly; amplitude perturbations were distributed normally. The noise perturbations within the simulated EEG data were scaled to create 32 levels of noise ranging from 0.4 to 10 times the standard deviation of the exemplar EEG data set in increments of 0.31 standard deviations. Simulated data constructed in this manner do not include eyeblink artifacts, and thus constitute the “ground truth” for ICA artifact correction. That is, this data can be compared with reconstructed data created by removing each ICA component. The reconstructed data that is most similar to the ground truth data must then reflect removal of the truly artifactual eyeblink component (as opposed to the other nonartifactual components).

Eyeblink artifacts were then introduced into the simulated data using a Chebyshev window (250 ms in length) as the model eyeblink. Twenty eyeblinks were introduced into the simulated time series at a rate of roughly one blink every 1.25 s with the propagation of the simulated blinks across the scalp controlled by a spherical head model derived empirically from the exemplar EEG data set. The simulated eyeblinks were scaled to create 32 levels of artifact magnitude ranging from 20 to 300 μV in increments of 9 μV. This approach therefore allowed for the examination of the automated eyeblink component selection algorithms across an extreme range of signal-to-noise ratios. Figure 2 provides exemplars of the

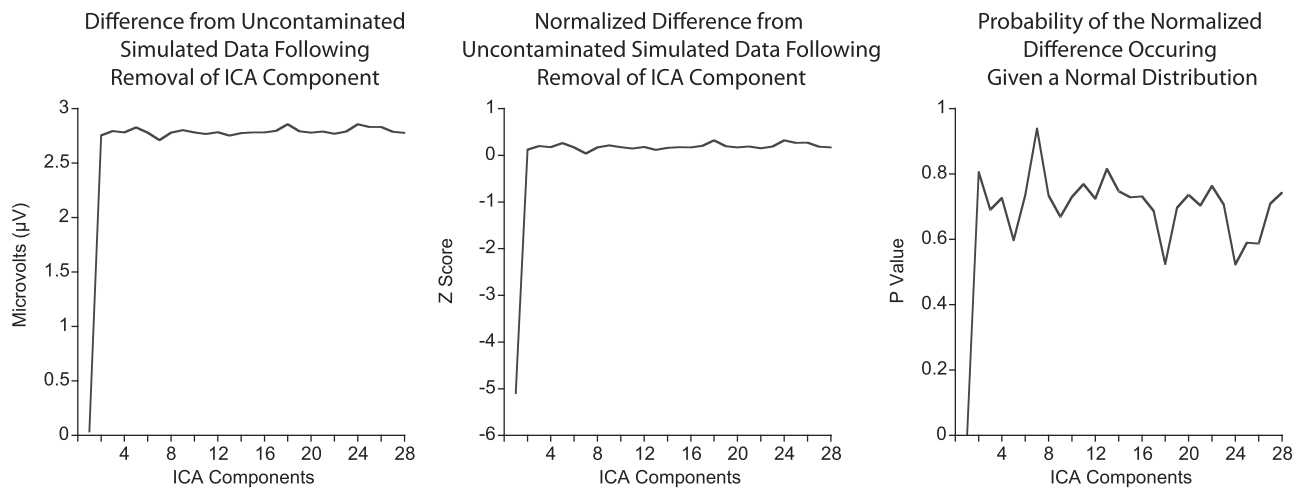


**Figure 3.** Representative data illustrating how the ground truth artifact-related ICA component was identified in the simulated EEG data. Only the removal of a single component returns the simulated data to near its uncontaminated state, with the normalized difference between the uncontaminated data and the contaminated data following removal of the ICA component reflecting that component as an outlier. As most components should be unrelated to the artifact, any component identified as an outlier was considered as related to the artifact.

simulated EEG across the range of possible eyeblink artifact magnitude and noise conditions.

Following each simulation, ICA decompositions were performed using the extended infomax algorithm to extract sub-Gaussian components using the default settings called for the binary instance of this function in EEGLAB. To identify the components related to the simulated artifact, the mean difference (as an absolute value) between the blink-free simulated data and the reconstructed simulated data was computed following back projection of the data without each ICA component, separately. As the eyeblink component(s)

should be rare relative to the other components, the truly artifactual components were selected by normalizing the differences and computing the probability of the difference occurring given a normal distribution (see Figure 3). Those components with a probability less than 0.05 were identified as truly artifactual components. Across the 3,072 simulations, the truly artifactual ICA component was identified in 1,700 (55.3%) of the simulations with instances where the truly artifactual component was unable to be determined occurring when the magnitude of the noise far exceeded the magnitude of the eyeblink (see Figure 2 and 4). Comparison of the

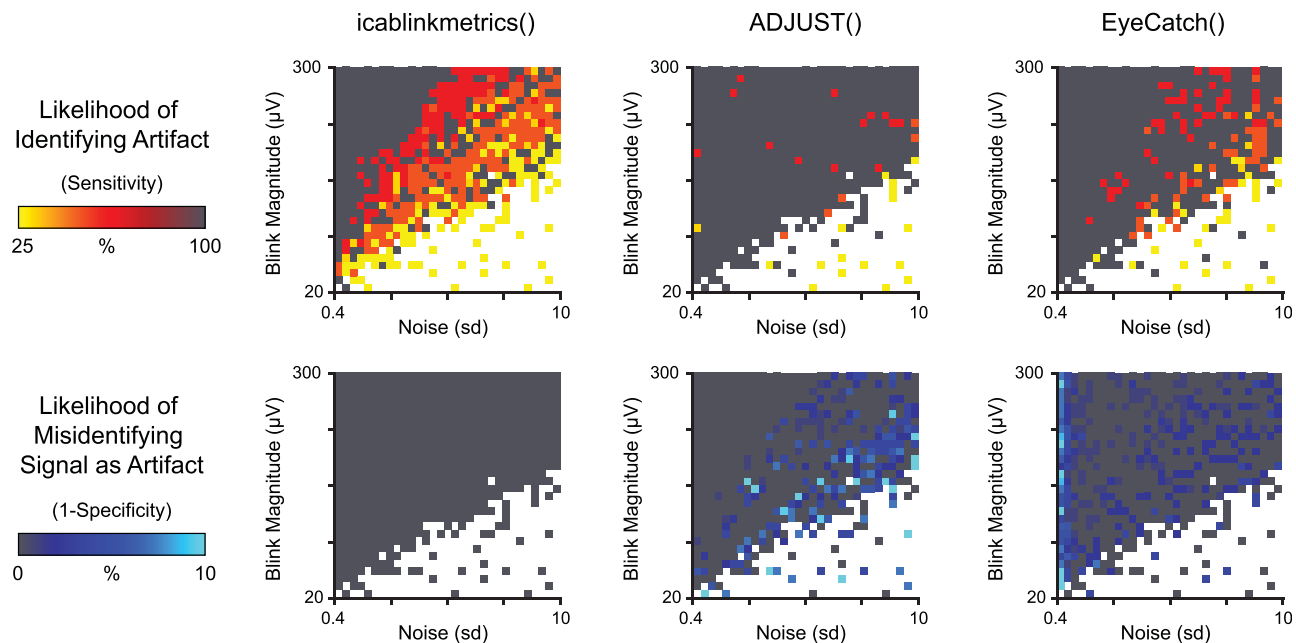


**Figure 4.** Graphic illustration of the results of 3,072 simulations of EEG data (1,024 simulations per exemplar data set) for the likelihood of identifying the artifact (sensitivity) and the likelihood of misidentifying signal as artifact (1-specificity) as a function of eyeblink magnitude and noise for each automated procedure. As each exemplar data set was used to test the full range of signal to noise, some data points may only reflect a singular simulation whereas others may reflect the result of three simulations at that eyeblink magnitude and noise level. Areas where the ground truth eyeblink component was unable to be determined (occurring in 1,372 of the 3,072) are uncolored.

**Table 1.** ICA Component Classifications

	True positive Eyeblink correctly classified (Rejected artifact)	True negative Nonblink correctly classified (Retained signal)	False positive Said it was eyeblink but it was not (Rejected signal)	False negative Said it was not an eyeblink but it was (Retained artifact)	Sensitivity TP/(TP + FN) (Identify artifact)	Specificity TN/(TN + FP) (Identify signal)	Reduction of artifact Based on components selected
<b>Simulated data</b>							
icablinkmetrics	1,234	45,900	0	466	72.6%	100%	89.5%
ADJUST	1,662	45,436	464	38	97.8%	99.0%	82.8%
EyeCatch	1,560	45,428	472	140	91.8%	99.0%	83.9%
<b>Real data</b>							
icablinkmetrics	92	4,936	0	0	100%	100%	88.0%
32-channel array	40	998	0	0	100%	100%	93.4%
64-channel array	38	2,233	0	0	100%	100%	89.3%
128-channel array	14	1,705	0	0	100%	100%	69.2%
ADJUST	89	4,738	198	3	96.7%	96.0%	86.6%
32-channel array	39	959	39	1	97.5%	96.1%	91.3%
64-channel array	38	2,110	123	0	100%	94.5%	88.7%
128-channel array	12	1,669	36	2	85.7%	97.9%	67.2%
EyeCatch	92	4,847	89	0	100%	98.2%	87.2%
32-channel array	40	950	48	0	100%	95.2%	93.3%
64-channel array	38	2,212	21	0	100%	99.1%	89.2%
128-channel array	14	1,685	20	0	100%	98.8%	64.1%
Expert observer	89	4,930	6	3	96.7%	99.9%	85.4%
32-channel array	38	994	4	2	95.0%	99.6%	88.9%
64-channel array	38	2,233	0	0	100%	100%	89.3%
128-channel array	13	1,703	2	1	92.9%	99.9%	64.6%
Competent observer	81	4,921	15	11	88.0%	99.7%	79.8%
32-channel array	38	994	4	2	95.0%	99.6%	88.9%
64-channel array	38	2,232	1	0	100%	100%	89.3%
128-channel array	5	1,695	10	9	35.7%	99.4%	27.7%
Novice observer	81	4,888	48	11	88.0%	99.0%	82.4%
32-channel array	38	977	21	2	95.0%	97.9%	89.0%
64-channel array	37	2,230	3	1	97.4%	99.9%	88.9%
128-channel array	6	1,681	24	8	42.9%	98.6%	46.0%

Note. Values indicate the number of components. The values for reduction of artifact indicate the percentage of the artifact removed following removal of the ICA components identified as artifactual. For the simulated data, this value reflects the percent similarity between the simulated data prior to the introduction of eyeblink artifacts and the reconstructed data following removal of the selected ICA components. For the real data, this value reflects the percent reduction of the convolution (i.e., overlap) between the mean eyeblink artifact and the EEG activity across all electrode sites during this same period following removal of the selected ICA components.

automated component selection procedures was restricted to only those simulations where the truly artifactual component was able to be identified.

Each of the three automated procedures (icablinkmetrics version 3.1, ADJUST version 1.1.1, and EyeCatch) was then tested using their default parameters. The icablinkmetrics function was run using the vertical electrooculogram (VEOG) channel of the simulated data set as the artifact comparison channel. The icablinkmetrics function identified eyeblinks within the artifact channel by cross-correlating a canonical eyeblink waveform using the eyeblinklatencies function, only accepting seeded eyeblinks that exhibited correlations of 0.96 or higher. Quantification of the efficacy of the automated component selection approaches for reducing the simulated artifact was performed by computing the percent reduction in the difference between the blink-free simulated data and the reconstructed simulated data ([absolute value([difference between data with simulated eyeblink and blink-free data] – [difference between reconstructed data following artifact removal and blink-free data])/ (difference between data with simulated eyeblink and blink-free data)]; see Table 1). Perfect reconstruction of the simulated data to its blink-free state would thus be reflected by 100% reduction in the difference between the blink-free simulated data and the reconstructed simulated data following artifact removal. All data

processing was conducted using an Apple iMac with a 3.5 GHz Intel Core i7 processor and 32 GB of 1600 MHz DDR3 SDRAM.

### Statistical Analysis

The efficacy of the automated procedures for identifying the eyeblink ICA component were examined statistically by evaluating their sensitivity (the likelihood of correctly identifying the eyeblink ICA component(s); i.e., hits) and specificity (the likelihood of correctly not identifying a nonblink component as an eyeblink ICA component(s); i.e., correct rejections) relative to the truly artifactual component. As all simulated data sets were contaminated by eyeblink artifact, failure to select an eyeblink component was considered a false negative error (miss), unless the truly artifactual component was unable to be determined (e.g., such as if the info-max algorithm was unable to separate the seeded eyeblink from the background noise).

### Results

Component selection counts along with the sensitivity and specificity are provided in Table 1. A graphic illustration of the likelihood of identifying the artifact (sensitivity) and the likelihood of

misidentifying signal as artifact (1-specificity) as a function of eyeblink magnitude and noise for each automated procedure is provided in Figure 4. Results of the simulation indicate that icablinkmetrics exhibited a lower sensitivity level (72.6%) than ADJUST and EyeCatch, which exhibited sensitivities above 91%. The sensitivity of icablinkmetrics and EyeCatch was observed to vary as a function of the magnitude of the eyeblink artifact and the relative noise level, with both demonstrating perfect sensitivity when the artifact amplitude-to-noise ratio was high. However, as the artifact amplitude-to-noise ratio was reduced, so too was the sensitivity (see Figure 4). In contrast, ADJUST exhibited a less interpretable pattern of decreases in sensitivity.

Although icablinkmetrics exhibited reduced sensitivity relative to the other methods, it also displayed perfect specificity (i.e., it never made any false alarms) regardless of the artifact amplitude or noise level of the simulated data. The specificity of ADJUST was observed to vary as a function of the magnitude of the eyeblink artifact and the relative noise level, demonstrating perfect specificity when the artifact amplitude-to-noise ratio was high. However, as the artifact amplitude-to-noise ratio was reduced, so too was the specificity (see Figure 4). In contrast, EyeCatch exhibited a less interpretable pattern of decreases in specificity, seeming to have a greater incidence of falsely identifying components as artifactual when the noise level was the lowest. Additionally, icablinkmetrics was observed to exhibit a 0% false discovery rate with the removal of the selected components, resulting in 89.5% similarity to the original blink-free simulated data, whereas ADJUST and EyeCatch were observed to exhibit false discovery rates of 21.8% and 23.2%, respectively, with removal of the selected components resulting in less than an 84% similarity to the original blink-free simulated data. However, when restricted to only those instances where all three automated component selection approaches were able to identify a component as artifactual—thereby ensuring equivalent comparisons free from potential bias related to the failure to identify a component—the components selected by icablinkmetrics, ADJUST, and EyeCatch were all observed to return the data with approximately 91% similarity to the original blink-free simulated data.

## Discussion

The aim of this section was to evaluate the extent to which automatic eyeblink ICA component selection methods would be sensitive to variation in the magnitude of the eyeblink artifact amid increasing levels of noise in the signal. Utilizing simulated EEG data with an identifiable, truly artifactual eyeblink ICA component revealed that, sensibly, decreases in the ratio between the artifact amplitude and the noise appeared to negatively impact each of the automated selection approaches. For the time series approach utilized by icablinkmetrics, decreases in the ratio between the artifact amplitude and the noise resulted in a reduced ability to identify a component as related to the artifact. However, despite alterations in the amplitude of the artifact and the noise, icablinkmetrics never falsely identified a nonartifactual component as related to the eyeblink. Under fully automated implementations then, icablinkmetrics might fail to identify ICA components associated with the eyeblink with noisier data sets but would seem to be robust against falsely removing signal-related ICA components (i.e., it errs on the side of caution), as reflected by a 100% positive predictive value and 99% negative predictive value.

EyeCatch in contrast, relying on spatial features alone, exhibited greater stability in its ability to identify eyeblink-related ICA

components despite decreases in the ratio between the artifact amplitude and the noise. However, EyeCatch exhibited the highest false discovery rate of any of the methods, particularly when the data set exhibited very low levels of noise, suggesting that under fully automated implementations EyeCatch might encourage the removal of signal-related ICA components—as reflected by 76.8% positive predictive value and 99.7% negative predictive value.

ADJUST, which relies on combined stereotypical spatial and temporal features, was observed to exhibit more random failures in the ability to identify ICA components associated with the eyeblink, whereas only the likelihood of falsely identifying signal-related ICA components was related to the ratio between the artifact amplitude and the noise. Thus, similar to EyeCatch, ADJUST exhibited a 78.2% positive predictive value and 99.9% negative predictive value suggestive of a bias toward detecting the eyeblink-related component at the expense of occasionally falsely identifying a signal-related component as artifactual. From a signal detection standpoint, these results are sensible; that is, the approach (icablinkmetrics) that made no false alarms also exhibited many misses, while the approaches (ADJUST and EyeCatch) that had the most hits also had the most false alarms.

To ensure that the eyeblink artifact is fully removed (e.g., in cases where the ICA algorithm separated the eyeblink artifact across multiple components), one might consider the bias to remove several ICA components a strength of the ADJUST and EyeCatch approaches. However, within the context of the present investigation, the ICA algorithm was effectively able to dissociate the eyeblink-related activity into a singular component. Thus, other components simply reflect random perturbations of the signal, and their removal would have little benefit for restoring the data to its original uncontaminated state. Indeed, when all three automated approaches returned component identifications, removal of additional components by the ADJUST and EyeCatch approaches provided no incremental improvement in restoring the data to its uncontaminated state, as all approaches exhibited approximately 91% similarity to the original data following removal of the identified components. Such false positive component identifications, however, may be more detrimental within real EEG data sets as the components selected for removal may be associated with important aspects of the neural signal rather than the artifact. Although the use of simulated data allows for determination of the extent to which these selection approaches can identify the truly artifactual component associated with the eyeblink, prior to recommending the utilization of any of these fully automated approaches, it is necessary to further examine their efficacy when used with real EEG data varying across common electrode densities (i.e., 32-, 64-, and 128-channel montages) and in response to different tasks. We address this issue next.

## Generalizability Across Electrode Densities Using Real EEG Data

### Method

All participants provided written informed consent in accordance with the Institutional Review Board at Michigan State University and at Binghamton University. The 32-channel data set included 40 participants (28 female; mean age =  $19.6 \pm 2.4$  years) who performed a go/no-go task with images of animals as targets while EEG was recorded (Laszlo & Sacchi, 2015). EEG was digitized at 500 Hz with an A/D (analog to digital) resolution of 16 bits and a software filter with a 10-s time constant and a 250 Hz low-pass

filter with a BrainAmp DC amplifier and a geodesically arranged electro-cap referenced online to the left mastoid and rereferenced offline to averaged mastoids. The VEOG was recorded using an electrode placed on the suborbital ridge of the left eye and referenced to the left mastoid.

The 64-channel data set utilized a sample of 38 participants (20 female; mean age =  $19.4 \pm 0.9$  years) who performed a perceptually challenging three-stimulus oddball task (Pontifex, Parks, Henning, & Kamijo, 2015) while EEG activity was recorded. Continuous data were digitized at a sampling rate of 1000 Hz and amplified 500 times with a DC to 70 Hz filter using a Neuroscan SynampsRT amplifier and a Neuroscan Quik-cap (Compumedics, Inc., Charlotte, NC) referenced to the CCPz electrode of the International 10/5 system (Jurcak, Tsuzuki, & Dan, 2007). Data were rereferenced offline to averaged mastoids. EOG activity was recorded from electrodes placed in a bipolar recording configuration above and below the orbit of the left eye.

The 128-channel data set utilized a sample of 14 participants (7 female; mean age =  $19.2 \pm 1.3$  years) who performed a free-viewing task involving 12 Hz ON/OFF luminance modulated photographs depicting complex, natural scenes while EEG activity was recorded. Continuous data were digitized at a sampling rate of 1000 Hz with 24-bit A/D resolution using the 400 Series Electrical Geodesics, Inc. (EGI) amplifier (DC to 100 Hz hardware filters) and a 129 HydroCel EEG net referenced to the Cz electrode. EOG activity was recorded from electrodes placed above the orbit of both eyes referenced to the Cz electrode.

These data sets, then, reflect not only diversity in how many electrodes were used, but also in what tasks were performed, how the VEOG was measured, and what configuration montage was used to place electrodes on the scalp. The sample data sets are thus well suited to addressing how generalizable the results of comparisons between the automated metrics might be to other real-world data sets.

## Procedure

For each data set, the EEG recordings were imported into EEGLAB and prepared for ICA decomposition. Data falling more than 2 s prior to the first event marker and 2 s after the final event marker were removed to restrict computation of ICA components to task-related activity. The data were then filtered using a 0.05 Hz high-pass IIR filter to remove slow drifts (Mognon et al., 2011). For the 32- and 64-channel data sets, EOG and mastoid (referential) electrodes were removed from the data and relocated in the EEGLAB EEG structure using movechannels, allowing for these electrodes to be restored following removal of the ICA artifact component(s) and the EOG electrodes to be available for use with the icablinkmetrics function.

ICA decompositions were performed using the extended infomax algorithm to extract sub-Gaussian components using the default settings called in the binary instance of this function in EEGLAB. Following the ICA computation, each of the three automated procedures (icablinkmetrics version 3.1, ADJUST version 1.1.1, and EyeCatch) were then tested using their default parameters. The artifact channel for icablinkmetrics was the VEOG channel in the 32- and 64-channel data sets, and channel 25 in the 128-channel EGI system. The icablinkmetrics function identified eyeblinks within the input artifact channel by cross-correlating a canonical eyeblink waveform using the eyeblinklatencies function, only accepting eyeblinks that exhibited correlations of 0.96 or higher. As the utilization of real data precludes knowing which

components are truly artifactual, components selected by the automated procedures were compared with those selected visually by an expert observer (SL) with 12 years of electrophysiology experience, who was blind to the selections made by any of the automated approaches. The expert observer followed current standard practice as described within EEGLAB documentation (Delorme & Makeig, 2004), which relies upon visual inspection of the scalp projection maps of the ICA components to make component selections. Thus, while the expert observer (SL) was involved in the creation of the icablinkmetrics algorithm,<sup>1</sup> in this manner the expert observer's approach was most similar to the EyeCatch algorithm. To ensure the integrity of the methodology, if the expert observer and automated procedures disagreed in their classification of components, a more thorough evaluation by an impartial third experienced electrophysiologist (VM, 10 years experience, who was not involved in the creation of any of the automated selection approaches) was conducted by considering the input from all sources and reinspecting the data to determine which (if any) were correct. This validation approach is similar to the approaches utilized when validating the ADJUST, CORRMAP, and EyeCatch plugins (Bigdely-Shamlo et al., 2013; Mognon et al., 2011; Viola et al., 2009). Quantification of the efficacy of the automated component selection approaches for reducing the eyeblink artifact were performed by computing the percent reduction in the convolution (i.e., overlap) between the mean eyeblink artifact in the EEG collapsed across all electrodes and the EEG activity collapsed across all electrodes during the same period following removal of the selected ICA components.

## Statistical Analysis

The efficacy of the automated procedures for identifying the eyeblink ICA component were examined statistically by evaluating their sensitivity (the likelihood of correctly identifying the eyeblink ICA component(s); i.e., hits) and specificity (the likelihood of correctly not identifying a nonblink component as an eyeblink ICA component(s); i.e., correct rejections) relative to the expert-selected component or components. As all data sets were contaminated by eyeblink artifact, failure to select an eyeblink component was considered a false negative error (miss).

## Results

The mean number of eyeblink artifacts present within the data for each participant was  $170.5 \pm 100.4$  (min: 32; max: 490) for the 32-channel data,  $107.9 \pm 71.6$  (min: 30; max: 326) for the 64-channel data, and  $61.1 \pm 39.9$  (min: 20; max: 140) for the 128-channel data. Computation of the independent components was performed using  $838.3 \pm 251.8$  data points for each ICA weight (data points/channels<sup>2</sup>) for the 32-channel data,  $152.9 \pm 13.4$  points for the 64-channel data, and  $35.4 \pm 3.0$  points for the 128-channel data. The mean time necessary for eyeblink identification and metric computation using icablinkmetrics was  $1.0 \pm 0.3$  s for each participant for the 32-channel data,  $3.3 \pm 1.2$  s for the 64-channel data, and  $7.4 \pm 4.0$  s for the 128-channel data. The mean time necessary for identification of components by the ADJUST and EyeCatch algorithms was  $2.2 \pm 0.6$  and  $3.1 \pm 0.1$  s for each participant for

<sup>1</sup> Though SL contributed to the design of icablinkmetrics, she was not responsible for actually implementing it and did not know what its behavior would be with respect to these data sets prior to making her selections.

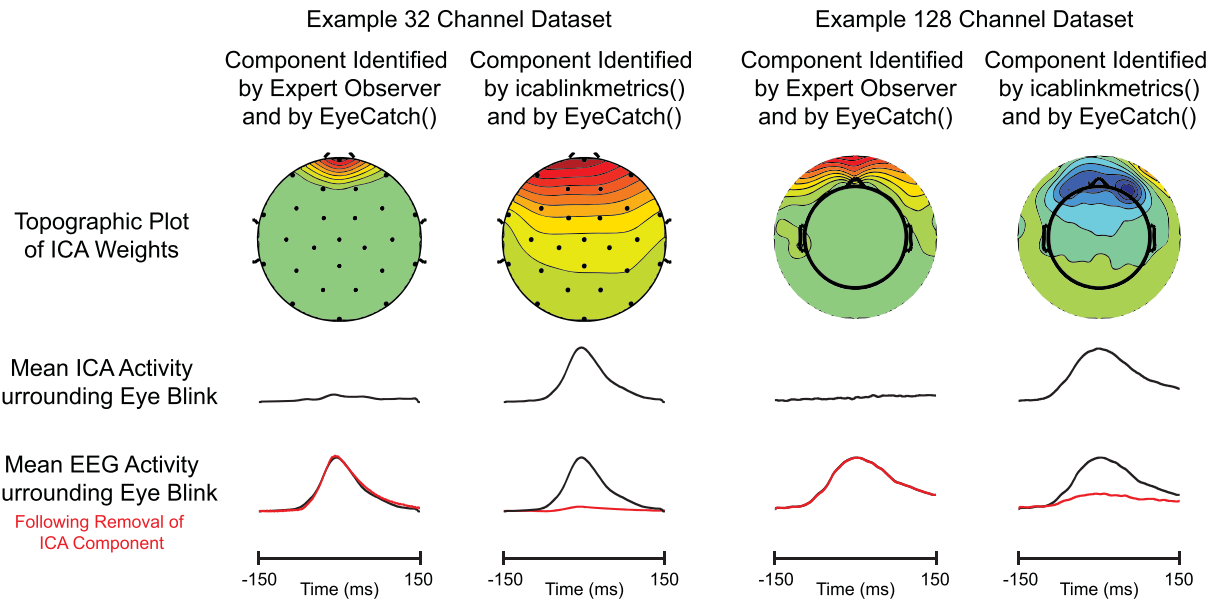


**Figure 5.** Two ICA components from a single participant recorded from a 32-channel montage and a single participant recorded from a 128-channel montage. EyeCatch identified all components as being related to the eyeblink, whereas the components on the left of each montage were identified by the expert observer and the components on the right of each montage were identified by icablinkmetrics. Note that, for both the example files, the ICA weights are frontally distributed for both components, but only a single component reduces the eyeblink artifact when the component is removed. As removal of the additional component has no influence over the mean blink-related activity, it can be considered as a false positive component identification.

the 32-channel data,  $4.1 \pm 0.2$  and  $6.3 \pm 2.4$  s for the 64-channel data, and  $8.2 \pm 0.4$  and  $14.5 \pm 0.8$  s for the 128-channel data, respectively, suggesting that icablinkmetrics is a slightly faster procedure overall.

Component selection counts along with the sensitivity and specificity are provided in Table 1. When utilizing real EEG data, all three automated procedures exhibited high levels of sensitivity in correctly identifying the eyeblink ICA component(s), with both icablinkmetrics and EyeCatch exhibiting perfect sensitivity. ADJUST in contrast, exhibited a sensitivity of 96.7%; failing to identify one eyeblink component in the 32-channel data set and two components in the 128-channel data set.

Although perfect sensitivity was observed for both icablinkmetrics and EyeCatch, only icablinkmetrics also exhibited perfect specificity (the likelihood of correctly not identifying a nonblink component as an eyeblink ICA component(s); i.e., correct rejections). EyeCatch falsely identified 89 components (48 from the 32-channel data set, 21 from the 64-channel data set, and 20 from the 128-channel data set) resulting in a false discovery rate of 49.2%. By comparison, ADJUST falsely identified 198 components (39 from the 32-channel data set, 123 from the 64-channel data set, and 36 from the 128-channel data set) resulting in a false discovery rate of 69%.

To gauge the extent to which removal of the ICA components selected as artifactual was effective in removing the eyeblink artifact from the EEG data, the percent reduction in the convolution (i.e., overlap) between the mean eyeblink artifact and the EEG activity across all electrode sites during this same period following removal of the selected ICA components was computed. The components selected by icablinkmetrics and EyeCatch were observed to reduce the eyeblink artifact present within the EEG by 88% and 87.2%, respectively, while the components selected by ADJUST were observed to reduce the eyeblink artifact by 86.6%.

## Discussion

The aim of this section was to evaluate the generalizability of these automated approaches across real EEG data sets. To this end, we utilized real EEG data recorded with variable numbers of sensors and in response to different experimental tasks. Further, each of the bioamplification systems from which data were submitted utilized a different recording configuration for EOG electrodes (bipolar, lower-orbit unipolar to mastoid, upper-orbit unipolar to vertex) and different acquisition parameters (e.g., acquisition filters, sampling rate, A/D resolution). Despite the substantial diversity in the data provided, icablinkmetrics demonstrated a high level of performance in automatically identifying the blink-related ICA components, exhibiting perfect sensitivity and specificity. Thus, while icablinkmetrics exhibited reduced sensitivity under noisy conditions in the simulated data, this noise level would seem to be above that which is normally encountered in real EEG data. The fact that icablinkmetrics was able to accurately identify eyeblink components regardless of the hardware used for data acquisition, EOG montage, EEG montage, or the task being performed by participants demonstrates its robustness and suggests that it may be suitable for use across a diverse set of data acquisition systems and across tasks.

EyeCatch similarly exhibited perfect sensitivity in detecting the eyeblink-related components across data sets. However, when using real EEG data, EyeCatch rejected a total of 89 nonblink-related ICA components (see Figure 5). Some caution is warranted in evaluating this outcome as the EyeCatch function does not presently offer the ability to differentiate identified eyeblink components from lateral eye movement components. Thus, it may be that some of these rejected components reflect truly artifactual, lateral eye movement components that were identified by EyeCatch but were not the focus of the present investigation. The performance of

EyeCatch on the real data is consistent with its performance on the simulated data, in that its high hit rate was accompanied by a relatively high false alarm rate.

Despite the popularity of the ADJUST automated selection routine, the function demonstrated performance below that of either the icablinkmetrics or EyeCatch. The poorer reduction in the eyeblink artifact present within the EEG is not surprising given that the ADJUST algorithm retained three artifact-related components while rejecting a total of 198 signal-related ICA components. Thus, it would appear that the criteria for identifying eyeblink-related ICA components utilized by the ADJUST function are neither as specific nor as sensitive as those used by the other automated component selection approaches.

At this point, we have compared the automated methods to each other, in both real and simulated data. However, we have not yet compared them to the commonly used practice wherein trained human observers visually select ICA components. Regardless of the interalgorithm comparisons, it would not be reasonable to recommend any of them if they cannot outperform a human observer. For this reason, we next evaluate the performance of trained observers with varying expertise levels in identifying artifactual ICA components in the real data sets used for algorithm comparison in this section.

### **Accuracy of Component Selection Relative to Trained Observers**

#### **Method**

The same real EEG data sets used above were used herein to enable comparisons between automated approaches and trained observers. The consensus-selected components identified above were compared here with those selected visually by electrophysiologists of varying experience (expert observer: 12 years [SL]; competent observer: 3 years; and novice observer: 2 years) who were blind to the selections made by any of the automated approaches. Trained observers had access to the complete EEG data set in EEGLAB to make their eyeblink component selections. Quantification of the efficacy of the trained observers for reducing the eyeblink artifact was performed by computing the percent reduction in the convolution (i.e., overlap) between the mean eyeblink artifact in the EEG collapsed across all electrodes and the EEG activity collapsed across all electrodes during the same period following removal of the selected ICA components.

#### **Statistical Analysis**

The efficacy of the trained observers in identifying the eyeblink ICA component were examined statistically by evaluating their sensitivity (the likelihood of correctly identifying the eyeblink ICA component(s); i.e., hits) and specificity (the likelihood of correctly not identifying a nonblink component as an eyeblink ICA component(s); i.e., correct rejections) relative to the consensus expert-selected component identified above (these were not necessarily always SL's selection, as she could have been overruled by consensus between VM and the automated approaches). As all simulated data sets were contaminated by eyeblink artifact, failure to select an eyeblink component was considered a false negative error (miss).

#### **Results**

Component selection counts along with the sensitivity and specificity are provided in Table 1. The percent agreement and Fleiss's kappa for the selection of the eyeblink component among the human raters was 95% agreement and 0.316 kappa for the 32-channel data set, 97.4% agreement and 0.49 kappa for the 64-channel data set, and 35.7% agreement with 0.125 kappa for the 128-channel data set.

The expert observer exhibited 96.7% sensitivity, failing to identify 2 eyeblink components in the 32-channel data set and 1 component in the 128-channel data set. Both the competent observer (with 3 years experience) and the novice observer (with 2 years experience) exhibited 88% sensitivity. The competent observer failed to identify 2 eyeblink components in the 32-channel data set, and 9 components in the 128-channel data set, while the novice observer failed to identify 2 eyeblink components in the 32-channel data set, 1 component in the 64-channel array, and 8 components in the 128-channel data set.

Regarding the specificity of the trained observers, even the expert observer incorrectly identified signal-related components as being related to the eyeblink, exhibiting 99.9% specificity (falsely identifying 6 components: 4 from the 32-channel data set, and 2 from the 128-channel data set) with a 6.3% false discovery rate. The competent observer exhibited 99.7% specificity (falsely identifying 15 components: 4 from the 32-channel data set, 1 from the 64-channel data set, and 10 from the 128-channel data set) with a 15.6% false discovery rate. The novice observer exhibited 99% specificity (falsely identifying 48 components: 21 from the 32-channel data set, 3 from the 64-channel data set, and 24 from the 128-channel data set) with a 37.2% false discovery rate.

#### **Discussion**

The aim of this section was to assess the accuracy of the commonly used method of trained observers visually selecting ICA components for comparison against the automated methods of eyeblink component selection. Across real EEG data varying in number of channels recorded and tasks performed, a clear trend was observed demonstrating the experience-dependent nature of visual component selection. The expert observer was able to correctly identify eyeblink components at 96.7% accuracy and rule out nonblink-related components at 99.9% accuracy. Inexperience was related to decreased accuracy, with 88% accuracy in identifying the eyeblink component for both the competent and novice observers, and 99.7% and 99% accuracy in ruling out nonblink-related components, for the competent and novice observers, respectively. This experience-dependent trend was most readily identifiable within the 128-channel data set, with the number of false discovery component identifications increasing with inexperience, whereas in the 32- and 64-channel data sets there was greater similarity between the expert and competent observers.

Although speculative, the experience-dependent nature observed within the 128-channel data set may be related to the scalp projection maps of the ICA components. A key differentiation between visual inspection of the topographic distribution of ICA weights for 32- and 64-channel data relative to 128-channel data is that, by default, EEGLAB does not plot the scalp projection maps the same way for the 128-channel plots relative to plots for lower-density arrays. Specifically, the plots are created for 128-channel data without electrode locations and with the activity extending beyond the circumference of the top of the head (as

illustrated in Figure 5). Less experienced electrophysiologists may rely on the electrode locations and reference points to a greater extent than more experienced electrophysiologists. Although the default settings were used within the present investigation, it should be noted that it is possible to include the electrode locations using the plotrad command in EEGLAB's topoplot function to potentially mitigate this issue. Another possible—though equally speculative—reason that there was a larger experience effect for the 128-channel data is that, because so many components are identified in the higher-density ICA computation, the actual eyeblink components are somewhat overfit. That is, spatial projections do not display as smooth a topography as the blink components in the lower density data. It may be that less experienced observers rely more on a smoother (less nuanced) template of what the blink artifact should look like, and are thus disproportionately distracted by the spatially overfit components produced in the high density data.

### Overall Discussion

Collectively, this investigation sought to determine the efficacy of fully automated approaches for selecting eyeblink-related temporal ICA components with a view toward understanding the potential utility of such approaches to replace the labor intensive (and potentially biased) process of human observers manually selecting components. To this end, we assessed the relative strengths of automatic eyeblink ICA component selection methods relying on time series data (icablinkmetrics) as compared to those relying on combined stereotypical spatial and temporal features (ADJUST, Mognon et al., 2011) or spatial features alone (EyeCatch, Bigdely-Shamlo et al., 2013). Three questions were then addressed; namely, (1) How robust are these approaches to variations in the magnitude of the eyeblink artifact amid increasing levels of noise in the signal using simulated EEG data? (2) How generalizable are these approaches across variable electrode densities and experimental tasks? (3) How do these approaches compare to the current common method of trained observers visually selecting temporal ICA components?

Relative to the first two questions, our findings suggest that, despite the popularity of ADJUST, its use of combined stereotypical spatial and temporal features resulted in more random failures in the ability to identify temporal ICA components associated with the eyeblink, irrespective of the ratio between the artifact amplitude and the noise when tested using simulated EEG data (Figure 4). When utilized with real EEG data, ADJUST was able to identify eyeblink-related components across electrode arrays at a similar level to that of the expert observer (96.7%). However, ADJUST greatly struggled in the specificity of the component selections exhibiting a false discovery rate of 69%. Thus, while ADJUST appears to be relatively robust and generalizable in its ability to identify eyeblink-related ICA components, signal-related temporal ICA components representing brain electrical activity may be mistakenly identified as artifact and rejected via the ADJUST approach—particularly when high levels of noise are present within the signal.

Relying on spatial features alone, EyeCatch was found to be sensitive to variation in the magnitude of the artifact amid increasing levels of noise, demonstrating both a decreased ability to identify eyeblink-related components when the artifact magnitude-to-noise ratio was low and an increased occurrence of mistakenly identifying signal-related components as artifact under low noise levels. More promisingly, in the real EEG data sets, EyeCatch exhibited perfect sensitivity in identifying eyeblink-related

components but struggled in mistakenly identifying signal-related components as artifact with a false discovery rate of 49.2%. The reduced specificity of EyeCatch was particularly prevalent for data recorded with lower-density electrode montages. Thus, EyeCatch was observed to be not particularly robust or generalizable in avoiding false discovery component identifications within the current investigation.

The time series approach utilized by icablinkmetrics was the least robust to variation in the amplitude of the artifact relative to increasing levels of noise, particularly struggling to identify the eyeblink component when the artifact was small relative to the level of background noise (see Figure 2). However, with the real EEG data, (where the signal-to-noise ratio was greater than the extremes utilized in the simulation data) icablinkmetrics exhibited perfect sensitivity across electrode montages and was observed to never falsely identify a component as being related to the eyeblink regardless of the use of real or simulated EEG. Thus, while icablinkmetrics was not observed to be robust in its sensitivity in identifying the artifact under increased levels of noise, it appears both robust and generalizable under more normal EEG recording conditions.

Relative to the third question of how these approaches compare to the current standard method of trained observers visually selecting temporal ICA components, all three methods of automatic component selection were able to accurately identify eyeblink-related ICA components at or above the level of human observers. Although the expert observer only failed to identify three blink components in the 93 real EEG data sets (see Figure 5), potentially more problematic was the finding that six ICA components were misidentified as being related to the eyeblink, meaning that six sources of nonartifactual signal would have been removed from the data (6.3% false discovery rate). Thus, even with substantial experience, signal-related temporal ICA components representing brain activity may be mistakenly identified as noise and rejected via the manual rejection approach. This trend is further magnified by expertise level, with the competent observer exhibiting a 15.6% false discovery rate and the novice observer exhibiting a 37.2% false discovery rate, while still retaining 11 artifact-related components. These findings call into question the extent to which the visual component identification approach using topographic projections of temporal ICA components should be considered the standard. Since visual component identification methods are time consuming and often considered “low-level” tasks, they are often relegated to less experienced users. Thus, given the substantially increased false discovery rates demonstrated by inexperienced raters, our findings highlight the reality that when student observers perform visual component identification they are very likely also removing signal-related temporal ICA components from the data, which may have substantial ramifications for the postprocessed EEG signal. Such an observation is particularly problematic given that only a small number of articles published in *Psychophysiology* over the past 2 years using ICA approaches for artifact correction have directly indicated using automated approaches for consistently determining components as artifact. In the absence of statements in the method, the assumption must therefore be that the vast majority of published literature utilizing the ICA approach for artifact correction has relied on human methods of component selection, which are not only resource intensive and slow but may also reduce the quality and integrity of the postprocessed EEG signal. Thus, the growing lack of replicability of findings within psychophysiology may very well relate, in some part, to the reliance on

human component selections in the increasing number of investigations utilizing ICA.

## Recommendations

As with any signal detection problem, these automated techniques must optimize their ability to identify the eyeblink-related component with their ability to correctly reject components not associated with the eyeblink. The use of simulated EEG data within the present investigation highlights a key difference between these automated component selection approaches in this matter. Both ADJUST and EyeCatch appear to be optimized toward identifying the eyeblink-related component at the cost of the occasional misidentification of a component—as evidenced by demonstrating poorer specificity than even a novice psychophysiologist; whereas icablinkmetrics is optimized toward correctly rejecting components not associated with the eyeblink at the cost of occasionally failing to identify the eyeblink-related component. However, it should be noted that such limitations were not observed with regard to the real EEG data—which fell within a less extreme range of signal-to-noise ratios than did the simulated data.

Accordingly, any means to utilize these approaches should thus acknowledge their respective limitations. Within the context of ADJUST and EyeCatch, these methods would seem better suited toward narrowing down potential candidate eyeblink components prior to human inspection. Given the superior performance of EyeCatch in detecting the eyeblink component within real EEG data, a recommendation for implementation would be to have the human observer make visual component selections from those temporal ICA components that were previously identified by EyeCatch. Rather than sifting through 30 or more components, this automated approach could be utilized to obtain a short list of candidate eyeblink components, serving to greatly reduce the potential burden and risk of false positive component identification associated with the trained observer approach.

Given the relative strengths of icablinkmetrics, which avoided false positive component identifications across the diverse data acquisition scenarios of the real EEG and the noisy simulated EEG data, it would seem that this approach is better suited toward a fully automated, user-independent implementation. As the icablinkmetrics approach either correctly identifies the eyeblink component or fails to identify any component, a recommendation for implementation would thus be to have the human observer only visually select components for those data sets where icablinkmetrics is unable to determine the eyeblink component. Rather than investing time inspecting all data sets, the human observer could instead focus on data sets that are particularly noisy or in which a bad channel was included in the temporal ICA decomposition, resulting in reduced quality of signal separation. The icablinkmetrics approach is ideally suited for such use as, in addition to outputting the identified component(s), it also outputs similarity metrics for the eyeblink artifact and each ICA component as well as the percent reduction in the eyeblink artifact observed when each ICA component is removed along with a graphic output for each ICA component—regardless of whether a component is identified as being artifactual. Accordingly, these metrics could be integrated alongside—rather than in lieu of—topographic projections of temporal ICA weights for those files in which an automatic solution cannot be resolved, or for those files in which visual identification of a component is especially difficult. Thus, in addition to being used as a means to automate the temporal ICA artifact correction approach, icablinkmetrics could be incorporated as a means of

ensuring a high level of confidence during visual selection of components, or to facilitate training of novice electrophysiologists. As recording of eyeblink-related activity seems to be falling out of favor with newer EEG acquisition systems, a potential weakness of the icablinkmetrics approach is specification of an electrode channel in which the eyeblink artifact manifests most clearly (e.g., the VEOG electrode) in order to construct a template of the eyeblink waveform for comparison with the ICA activations. However, it should be noted that any electrode could be used so long as the electrode specified captures the artifact of interest; in the absence of a VEOG electrode per se, several frontal or temporal electrodes would seem to be reasonable alternatives.

Although the present investigation did not assess the efficacy of these automated approaches for handling nonblink-related artifacts, it is worth noting that roughly half of the published literature in *Psychophysiology* over the past 2 years indicates only correcting for eyeblink-related artifact when using either regression- or ICA-based approaches. Ultimately, however, the context of the EEG recording necessarily dictates the nature and degree of artifact present within the data as some protocols may differentially manifest eyeblinks, saccadic eye movements, and muscle and cardiac-related artifacts. While it is clear that investigators are increasingly turning to ICA-based approaches for artifact correction, it is important to emphasize that there is no single best method for correcting all artifacts (Urigüen & Garcia-Zapirain, 2015). ICA-based approaches have been found to be particularly effective for correcting eyeblink-related artifacts (Jung et al., 2000). By comparison, regression-based approaches may be more appropriate for other artifacts such as saccadic eye movements and nonstationary artifacts (Hoffmann & Falkenstein, 2008). Based on the current state of the art, an ideal approach may be to implement artifact correction/suppression procedures across multiple processing stages, thereby enabling an investigator to use the best tool for each specific type of artifact (Urigüen & Garcia-Zapirain, 2015). Indeed, the use of ICA and regression-based approaches for artifact correction are not inherently mutually exclusive. Given the relative strengths and weaknesses of these methods (Hoffmann & Falkenstein, 2008), a temporal ICA approach to eyeblink artifact correction could be combined with existing regression-based approaches for the correction of other nonblink-related artifacts.

In considering the automated selection of temporal ICA components, it is important to note that a limitation of the present investigation is that the efficacy of these automated approaches may vary based upon the particular characteristics of the artifact of interest. Artifacts that exhibit temporally consistent morphological characteristics (such as eyeblink and electrocardiogram artifacts) would seem well suited for correction using temporal approaches to component identification. In such instances, the stationarity of the artifact produces a cleaner isolation and is ideally suited for time-domain approaches to component selection since the individual artifacts temporally align with the artifactual component(s). However, other nonstationary artifacts (such as saccadic eye movements) may be better suited for spatial approaches to component identification or for regression-based artifact correction procedures (Hoffmann & Falkenstein, 2008).

## Conclusions

Collectively, the present investigation demonstrated the efficacy of utilizing automated approaches for temporal ICA eyeblink

artifact selection, and compared automated approaches directly with human selection of eyeblink components among psychophysicists with a range of expertise. All of the automated methods assessed were good enough at identifying artifactual components to be considered as candidates for supplementing or replacing manual inspection. However, icablinkmetrics, in particular, would seem to provide

an effective means of automating eyeblink correction using temporal ICA, while at the same time eliminating human errors inevitable during manual component selection and false positive component identifications common in other automated approaches, given its exceptional specificity in all cases.

## References

- Bell, A. J., & Sejnowski, T. J. (1995). An information maximisation approach to blind separation and blind deconvolution. *Neural Computation*, *7*, 1129–1159. doi: 10.1162/neco.1995.7.6.1129
- Bigdely-Shamlo, N., Kreutz-Delgado, K., Kothe, C., & Makeig, S. (2013). EyeCatch: Data-mining over half a million EEG independent components to construct a fully-automated eye-component detector. *Annual International Conference of the IEEE Engineering in Medicine and Biology Society* (pp. 5845–5848). Piscataway, NJ: IEEE Service Center. doi: 10.1109/EMBC.2013.6610881
- Castellanos, N. P., & Makarov, V. A. (2006). Recovering EEG brain signals: Artifact suppression with wavelet enhanced independent component analysis. *Journal of Neuroscience Methods*, *158*, 300–312. doi: 10.1016/j.jneumeth.2006.05.033
- Delorme, A., & Makeig, S. (2004). EEGLAB: An open source toolbox for analysis of single-trial EEG dynamics. *Journal of Neuroscience Methods*, *134*, 9–21. doi: 10.1016/j.jneumeth.2003.10.009
- Hoffmann, S., & Falkenstein, M. (2008). Correction of eye blink artefacts in the EEG: A comparison of two prominent methods. *PLOS One*, *3*, 1–11. doi: 10.1371/journal.pone.0003004
- Jung, T., Makeig, S., Humphries, C., Lee, T., McKeown, M. J., Iragui, V., & Sejnowski, T. J. (2000). Removing electroencephalographic artifacts by blind source separation. *Psychophysiology*, *37*, 163–178. doi: 10.1111/1469-8986.3720163
- Jurcak, V., Tsuzuki, D., & Dan, I. (2007). 10/20, 10/10, and 10/5 systems revisited: Their validity as relative head-surface-based positioning systems. *NeuroImage*, *34*, 1600–1611. doi: 10.1016/j.neuroimage.2006.09.024
- Laszlo, S., & Armstrong, B. C. (2014). PSPs and ERPs: Applying the dynamics of post-synaptic potentials to individual units in simulation of ERP reading data. *Brain and Language*, *132*, 22–27. doi: 10.1016/j.bandl.2014.03.002
- Laszlo, S., & Plaut, D. C. (2012). A neurally plausible parallel distributed processing model of event-related potential word reading data. *Brain and Language*, *120*, 271–281. doi: 10.1016/j.bandl.2011.09.001
- Laszlo, S., & Sacchi. (2015). Individual differences in involvement of the visual object recognition system during visual word recognition. *Brain and Language*, *145*, 42–52. doi: 10.1016/j.bandl.2015.03.009
- Mognon, A., Jovicich, J., Bruzzone, L., & Buiatti, M. (2011). ADJUST: An automatic EEG artifact detector based on the joint use of spatial and temporal features. *Psychophysiology*, *48*, 229–240. doi: 10.1111/j.1469-8986.2010.01061.x
- Pontifex, M. B., Parks, A. C., Henning, D. A., & Kamijo, K. (2015). Single bouts of exercise selectively sustain attentional processes. *Psychophysiology*, *52*(5), 618–625. doi: 10.1111/psyp.12395
- Urigüen, J. A., & Garcia-Zapirain, B. (2015). EEG artifact removal—State-of-the-art and guidelines. *Journal of Neural Engineering*, *12*, 1–23. doi: 10.1088/1741-2560/12/3/031001
- Viola, F. C., Thorne, J., Edmonds, B., Schneider, T., & Eichele, T. (2009). Semi-automatic identification of independent components representing EEG artifact. *Clinical Neurophysiology*, *120*, 868–877. doi: 10.1016/j.clinph.2009.01.015

(RECEIVED March 24, 2016; ACCEPTED December 13, 2016)

## Supporting Information

Additional supporting information may be found in the online version of this article:

**Appendix S1:** Additional information about the background and theory underlying icablinkmetrics.

**Figure S1:** Comparison of ICA components across electrode arrays for the icablinkmetrics approach.

**Figure S2:** Visualization of the icablinkmetrics approach.